# A Belief Propagation Based Power Distribution System State Estimator

***Abstract***–The most popular method used in traditional power system state estimation is the Maximum Likelihood Estimation (MLE). It assumes the state of the system is a set of deterministic variables and determines the most likely state via error included interval measurements. In the distribution system, the measurements are often too sparse to fulfill the system observability. Instead of introducing pseudo-measurements, we propose a Belief Propagation (BP) based distribution system state estimator. This new approach assumes that the system state is a set of stochastic variables. With a set of prior distributions, it calculates the posterior distributions of the state variables via real-time sparse measurements from both traditional measurements and the high resolution smart metering data.

In this paper we discuss the step-by-step method of applying the BP algorithm on the distribution system state estimation problem. Our approach provides a seamless connection from the monitoring of transmission system to the feeder circuit, thus filling in the gap between the traditional energy management system (EMS) and the micro-grid customer level optimization. Furthermore, the proposed state estimator can not only be applied to the multi-level electrical coupled grid, but also accommodate the spatial-temporal model for the correlated distributed renewable energy resources. It provides a way of integrating the distributed renewable energy management system into the Smart-Grid Distribution Management System (DMS) and automated substations.

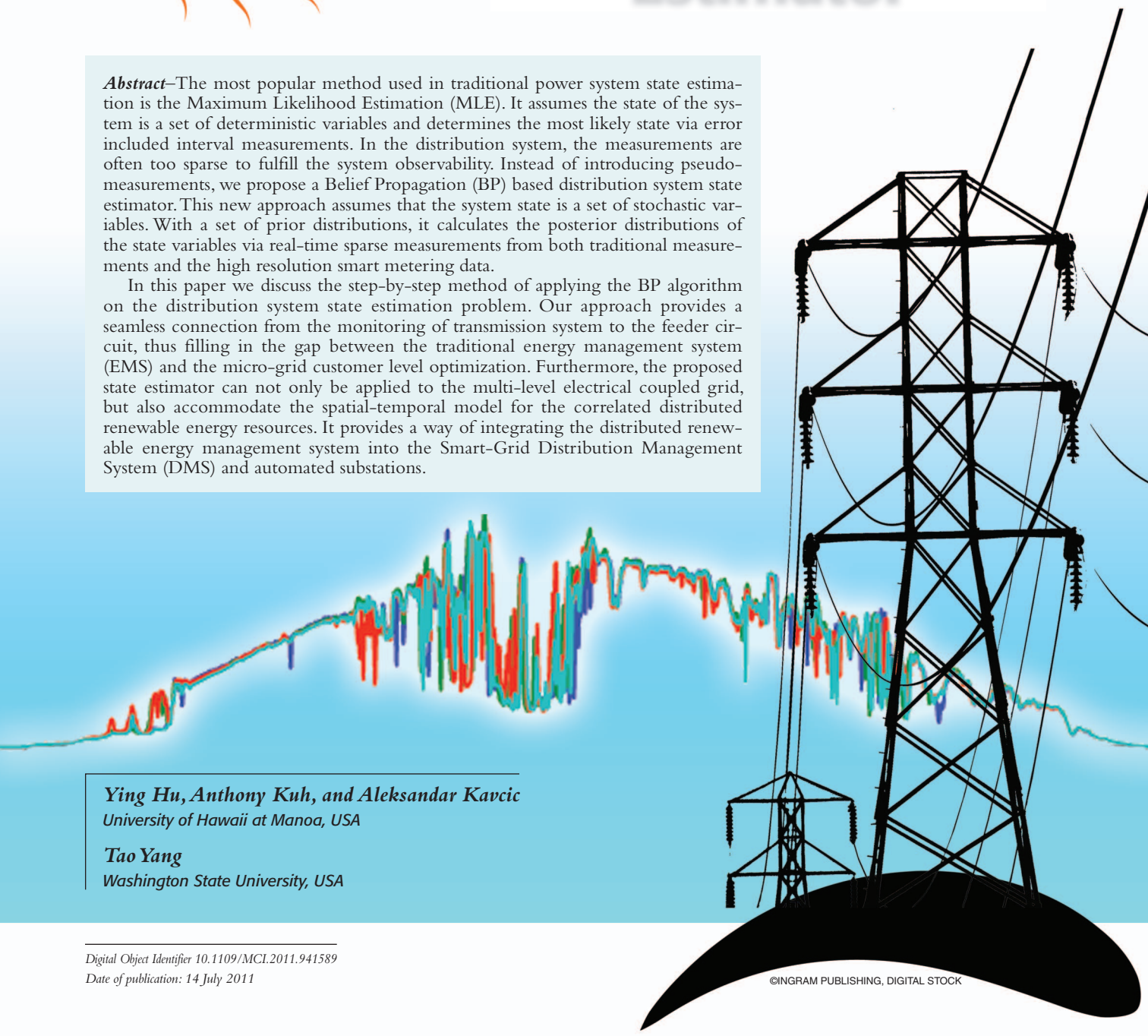

*Ying Hu, Anthony Kuh, and Aleksandar Kavcic*
*University of Hawaii at Manoa, USA*

*Tao Yang*
*Washington State University, USA*

*Digital Object Identifier 10.1109/MCI.2011.941589*
*Date of publication: 14 July 2011*





1556-603X/11/$26.00©2011IEEE

## I. Introduction

Traditional power system state estimator often uses the Weighted Least Square (WLS) algorithm which is based on Maximum Likelihood Estimation (MLE). In most cases, the real-time measurements are the combination of active power, reactive power, voltage and current magnitude. The measurement errors are assumed to be modeled as independent Gaussian random variables [1]. In the distribution grid, many features are different from the transmission grid such as the topology, mixture of three phases and single phase, and measurement redundancy. Approaches on distribution system state estimation are developed in [2]–[5] which can address these differences. In the distribution grid real-time measurement redundancy is not as high as in the transmission grid, therefore lots of pseudo-measurements are generated from historical data which are then used in distribution system state estimation to guarantee system observability [6]–[11].

Real-time measurements and pseudo-measurements are deterministic values in the state estimation procedure when using MLE algorithm. Correspondingly the system states are defined to be variables with hidden deterministic quantities. This is reasonable for transmission grids as in most cases the system is overdetermined by redundant real-time measurements. Furthermore, metering devices such as phasor measurement units (PMUs) that deliver synchrophasor measurements are being deployed and becoming more common in the transmission grid. To obtain a more accurate system state, state estimator can be incorporated with these high resolution measurements [12]. The percentage of pseudo-measurements is relatively small and would not affect the accuracy of the estimation.

In the distribution grid, real-time measurements are sparsely distributed thus lots of pseudo-measurements need to be introduced into the measurement set. The state estimation accuracy could be affected by the higher percentage of pseudo-measurements and because of uncertainties in the measurements we model these measurements as random variables. Hence in the distribution system it is reasonable to treat the system states as stochastic variables and use a probabilistic inference approach to construct the state estimation problem. Historical data are used to generate prior distribution of the states instead of deterministic pseudo-measurements.

In this paper, we use a Bayesian network to model the distribution system state estimation problem. A factor graph representing the distribution system is described. In the graphical model we define all the state variables and their probabilistic dependencies, which include both the electrical correlation and the environmental correlation due to the integration of renewable energy generation (REG). We use the Belief Propagation (BP) algorithm to conduct statistical inference. The state estimates are the marginal posterior distribution of the variable nodes.

We will show the convenience and efficiency of constructing a two-level architecture for the distribution network topology and applying the BP based state estimation at each level. With the development of digital substations with enhanced data processing ability [13], state estimation at the substation level can potentially enable real-time feeder analysis. The state estimates at the substation level can then be incorporated into the subtransmission system state estimator to avoid data communication burden. In a similar manner distribution system state estimation can be incorporated with transmission system state estimation as well.

This paper is organized as follows. In Section II we discuss Bayesian networks and the Belief Propagation (BP) algorithm. Section III discusses the factor graph model applied to microgrid estimation. This includes state variables, electrical correlations, and environmental correlations. Section IV discusses the BP based state estimator and implementation by applying it to a two-level distribution network. Section V shows a simplified example of a distribution feeder circuit and Section VI summarizes this paper and discusses further directions for this research.

## II. Bayesian Network and Belief Propagation

### *A. Bayesian Network*

A Bayesian network is a probabilistic graphical model that represents a set of random interactions [14] [15]. It has been applied in many computational intelligence and machine learning areas [15] [16]. The power grid can be naturally modeled as a Bayesian network as the electrical connections satisfy the local Markov property. We define state vectors to be the variable nodes on the Bayesian network model. State variables can be either observed via measurements from metering devices or are hidden states modeled as random variables. Note that this definition is different from the traditional state estimation where state variables have unknown deterministic values and can be computed based on the measurement set.

Bayesian network expresses a factorization of the joint probability distribution that is suitable to be represented by a factor graph [17]. Factor graph is an alternative graphical representation of probabilities that addresses the intermediate factors [18]. In the factor graph representation, factor nodes represent the correlation among variable nodes. The variable and factor nodes together form a bipartite graph and their connections are usually specified through an adjacency matrix.

In terms of modeling the power grid, a factor graph can not only capture the electrical correlation on the grid but also address other mathematical models, such as the renewable energy correlation and a load forecast model. With the factor graph model, a state estimator can be expanded with statistical models by simply introducing new factors. In Section III.C the correlation among the REG will be discussed based on the least squares fit of historical data. The spatial/temporal correlation model can be implemented as a factor function which exerts additional constraints on the corresponding state variables.

**In terms of modeling the power grid, a factor graph can not only capture the electrical correlation on the grid but also address other mathematical models, such as the renewable energy correlation and a load forecast model.**

Because the Bayesian network is a directed acyclic graphical model for the variables and their relationships, it can be used to compute the posterior distribution of variables given evidence (i.e. the probabilistic inference) [19] [20]. There are different kinds of inference methods such as the elimination algorithm and the sum-product algorithm. The Belief Propagation algorithm, also referred to as the sum-product algorithm, will be used in the proposed state estimator.

### *B. Belief Propagation*

The Belief Propagation algorithm is a message passing algorithm for computing the marginal distribution. It was first formulated on trees or tree-like structures, where the algorithm can derive exact marginals. Messages are real valued functions which are passed along the edges between the variable nodes. They represent the influence that one variable exerts on its parent/descendent variable. There are two types of messages on a factor graph as shown in Fig. 1.

- The message from a variable node $i$ to a factor node $s$:

$$m_{i\to s}(x_i) = \varphi_i(x_i) \prod_{g\in N(x_i):g\neq s} m_{g\to i}(x_i), \tag{1}$$

where $N(x_i)$ denotes all the neighboring factor nodes of $x_i$.

- The message from a factor node $s$ to a variable node $j$:

$$m_{s\to j}(x_j) = \sum_{x_i\in N(s):i\neq j} \left( s(N(s)) \prod_{i:i\neq j} m_{i\to s}(x_i) \right), \tag{2}$$

where $s(N(s))$ denotes function $s$ whose arguments are all the nodes in the set $N(s)$. $\varphi_i(x_i)$ is the evidence potential of $x_i$ given possible observation.

Reference [21] derived the message update rules for three linear building blocks as factor functions when the messages are Gaussian distributions.

Messages are passed in an order such that a node sends a message to a neighboring node only when it has received messages from all of its other neighbors [15]. Upon completion of the message passing, the marginal distribution of every variable node can be found from Eq. 3.

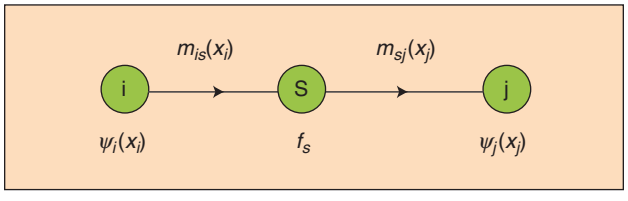


**FIGURE 1** Two types of messages.

$$P_{X_j}(x_j) = \varphi_j(x_j) \prod_{s\in N(j)} m_{s\to j}(x_j). \tag{3}$$

We adopt the additive white Gaussian noise (AWGN) model for noisy observations [23]. At time $t$ an observation $\gamma_t$ for the hidden state $x_t$ satisfies Eq. 4.

$$\gamma_t = x_t + z_t, \tag{4}$$

where $z_t$ is the observation noise and $z_t \sim N(0, R)$, Gaussian with zero mean and covariance matrix $R$.

The loopy BP algorithm is then developed to approximate inference on general graphs which typically contain loops. From empirical studies on the behavior of loopy BP, the algorithm often converges close to the true marginals. The same set of computation rules are deployed as in the BP algorithm. Since there are no specifications of leaves and roots on loopy graphs, the schedule of message passing is changed and summarized below [22]:

Suppose $E$ is the set of all variables nodes and $F$ is the set of all factors nodes.

1) For every variable $i$, initialize $m_{if}^1$ with the evidence potential $p_i(x_i)$ given possible observations.
2) While the stop criteria is not met,
   - For every $f \in F$, update messages $m_{fj}^{t+1}$ flowing from factor $f$ to all of its neighboring variables $j$ at time $t+1$ according to $m_{if}^t$.
   - For every $i \in E$, update messages $m_{if}^{t+1}$ flowing from variable $i$ to all of its neighboring factors $f$ at time $t+1$ according to $m_{gi}^{t+1}$.
3) Compute marginals $P_{X_i}(x_i)$ according to the steady state messages $m_{fi}$.

For simplicity we assume Gaussian distributions for all the state variables. In this case, messages only need to include the mean vector and the covariance matrix. The first and second order statistics can completely determine the pdf of corresponding variables. The Bayesian inference is conducted through the Gaussian BP algorithm which adopts the message passing rules of the loopy BP algorithm.

## III. Factor Graph Model

### *A. State Vector*

Traditional state estimation utilizes measurements from the supervisory control and data acquisition (SCADA) and automated meter reading (AMR) systems. With increasing amount of advanced metering infrastructure (AMI) and Phasor Measurement Units (PMU) being installed on respectively the distribution and transmission grid, data with high accuracy and very short sampling interval can potentially improve the performance of the state estimation. The BP based state estimator can process the two kinds of measurements simultaneously.

The available measurements may include branch power, power injection, bus voltage, branch current and current injection, etc. We choose the state variables to include

❏ Complex bus voltage $V$
❏ Complex branch current $Ib$
❏ Complex injection current $Ij$.

In the graphical model every state variable can be represented by a vector including the real and imaginary parts.

$$V_i = \begin{pmatrix} V_{i,\text{real}} \\ V_{i,\text{imag}} \end{pmatrix}, \quad Ib_i = \begin{pmatrix} Ib_{i,\text{real}} \\ Ib_{i,\text{imag}} \end{pmatrix}, \quad Ij_i = \begin{pmatrix} Ij_{i,\text{real}} \\ Ij_{i,\text{imag}} \end{pmatrix}. \tag{5}$$

The spatial/temporal correlation of the REG is involved with active and reactive power output from the renewable resources. In order to include the renewable correlation in the factor graph, we define the state variable for the branch associated with the REG to be the active and reactive power injection:

$$S_i = \begin{pmatrix} P_i \\ Q_i \end{pmatrix}. \tag{6}$$

The real-time estimates of the REG can be directly shown with the state estimator which properly integrates the spatial/temporal correlation among neighboring REG. Rather than simply viewing the REG as negative load, the state estimator can contribute this information to the distributed renewable energy management system.

Every variable node in the factor graph represents a state vector consisting of two state variables. When the variable node $X_i$ is not associated with the REG, the corresponding state vector is

$$X_i = \begin{bmatrix} V_{i,\text{real}} & I_{i,\text{real}} \\ V_{i,\text{imag}} & I_{i,\text{imag}} \end{bmatrix}, \tag{7}$$

where $V_i$ is the upstream bus voltage of branch $i$ and $I_i$ is the current flowing through branch $i$. For the variable node $X_j$ which includes power flow from the REG, the state vector is

$$X_j = \begin{bmatrix} V_{j,\text{real}} & P_j \\ V_{j,\text{imag}} & Q_j \end{bmatrix}. \tag{8}$$

In most cases power distribution circuits are radial, which results in radial factor graph with the above definitions of state vectors. The connection between variable nodes is determined by either the electrical connection among neighboring branches or their environmental correlation.

### *B. Electrical Correlation*

We used two factor function blocks to represent the electrical relationship on the circuit: $f_E$ and $f_L$. Every factor function in the factor graph consists of the two building blocks. When only voltage and current are considered in state estimation, all the circuit equations are linear thus a linear state estimator is sufficient. The active and reactive power can be calculated from the estimates of voltage and current in the post-calculation process.

However if the correlation among the REG is considered, the circuit equations need to include power injections at the switches which connect the REG to the grid. The corresponding nonlinear correlation function needs to be linearized so that all the messages can follow the same set of linear computation rules. With the linear approximation of the nonlinear correlations [23], the inference algorithm can converge to the optimal estimates after a certain number of iterations.

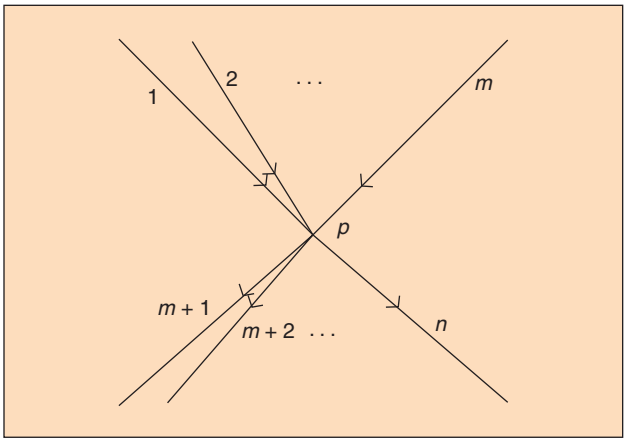


**FIGURE 2** The one-line diagram for a bus connected with branches.

#### **B.1** $f_E$

At all the buses, the currents need to satisfy the Kirchhoff Current Law (KCL). Suppose that branch $1, 2, \ldots, m$ have currents flowing to the bus $p$ and branch $m+1, \ldots, n$ have currents flowing from the bus $p$, as shown in Fig. 2.

According to KCL, Eq. 9 defines the factor function $f_E$.

$$\begin{cases} \sum_{i=1}^{m} Ib_{i,\text{real}} = \sum_{i=m+1}^{n} Ib_{i,\text{real}} \\ \sum_{i=1}^{m} Ib_{i,\text{imag}} = \sum_{i=m+1}^{n} Ib_{i,\text{imag}} \end{cases}. \tag{9}$$

For the bus with injection current, which usually represents the load or the REG, Fig. 3 shows the one-line diagram for illustrating the KCL at the bus.

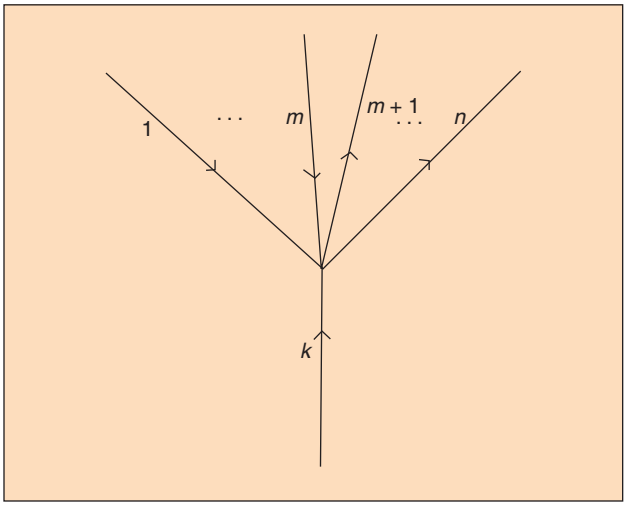


**FIGURE 3** The one-line diagram for a bus with injection current $Ij_k$.

**It is important to obtain good forecasts of wind and solar energy so that more accurate estimates can be obtained of grid parameters in order for good control strategies to be implemented.**

The factor function $f_E$ for the load injection bus is defined by Eq. 10.

$$\begin{cases} \sum_{i=1}^{m} Ib_{i,\text{real}} + Ij_{k,\text{real}} = \sum_{i=m+1}^{n} Ib_{i,\text{real}} \\ \sum_{i=1}^{m} Ib_{i,\text{imag}} + Ij_{k,\text{imag}} = \sum_{i=m+1}^{n} Ib_{i,\text{imag}} \end{cases}. \tag{10}$$

For the bus associated with the REG, the complex power flow along the injection branch as a state variable results in nonlinear equations. The corresponding factor function $f_E$ is defined by Eq. 11.

$$\sum_{i=1}^{m} Ib_i + \left(\frac{S_k}{V_k}\right)^* = \sum_{i=m+1}^{n} Ib_i. \tag{11}$$

After linear approximation, $S_k$ can be expressed as Eq. 12.

$$S_k \approx \left(\sum_{i=m+1}^{n} I\bar{b}_i^* - \sum_{i=1}^{m} I\bar{b}_i^*\right) V_k + \bar{V}_k \sum_{i=m+1}^{n} (Ib_i^* - I\bar{b}_i^*) - \bar{V}_k \sum_{i=1}^{m} (Ib_i^* - I\bar{b}_i^*), \tag{12}$$

where $I\bar{b}_i^*$ represents the mean of $Ib_j^*$ in the previous iteration of the state estimation algorithm. The equations for $P_k$ and $Q_k$ can be easily derived based on Eq.12.

**B.2** $f_L$

The factor function $f_L$ describes the electrical relationship across the impedance. Since the distribution lines are usually short (within 50 miles), we can simply model the line as an impedance $Z = R + jX$. In steady state analysis, transformers will be considered as a simple two-port network model. In the case where there is no phase shifting and tap changing, we can view the transformer as an impedance. Therefore the following set of equations can be applied to both distribution line model and transformer model:

$$\begin{cases} V_{u,\text{real}} - V_{d,\text{real}} = RIb_{i,\text{real}} - XIb_{i,\text{imag}} \\ V_{u,\text{imag}} - V_{d,\text{imag}} = RIb_{i,\text{imag}} + XIb_{i,\text{real}} \end{cases}, \tag{13}$$

where $V_u$ is the upstream bus voltage of branch $i$ and $V_d$ is the downstream bus voltage.

### *C. Environmental Correlation*

A key reason why we are studying state estimation at the distribution level is because of the introduction of distributed renewable energy sources such as wind and solar. These energy sources are intermittent and a high penetration of distributed renewable energy sources will affect the stability of the grid at the distribution level. Power balancing and voltage control is needed to stabilize the grid. Before this can be done we need to use state estimation to accurately estimate voltage and current at node locations on the grid.

It is important to obtain good forecasts of wind and solar energy so that more accurate estimates can be obtained of grid parameters in order for good control strategies to be implemented. In this subsection we conduct a preliminary study of prediction of solar insolation or incident solar radiation as solar electric power is directly proportional to insolation [24]. Using small scale solar photovoltaics (PV) generation at the Kilowatt level (at the distribution level on homes and buildings) has become increasingly more popular. As PV costs become more competitive with respect to the cost of conventional electricity generation, the percentages of distributed PV generation on homes and buildings will increase dramatically, necessitating good modeling of solar insolation both spatially and temporally.

We constructed a discrete time spatial-temporal model of solar insolation. We made the assumption that we have $n$ sensors measuring solar insolation. These sensors are placed at different geographic locations. We used signal processing methods to perform prediction for solar-insolation. Let $Y(k)$ be an $n$-vector with the $i$th component $Y_i(k)$ describing the solar insolation in Kilowatts/$m^2$ of sensor $i$ at time $k$. We would like to understand the effects of both temporal and spatial correlations on the solar insolation. The solar insolation process is a nonstationary process, but we started with simple models to begin to understand the behavior of the solar insolation process. We start by modeling the solar insolation process as a vector autoregressive (VAR) process described by

$$Y(k) = \sum_{i=1}^{p} A_i Y(k-i) + V(k),$$

where $A_i$ is an $n$ by $n$ matrix of real coefficients and $V(k)$ is an iid vector Gaussian process with mean $m_{v(k)}$ and covariance matrix $\Lambda_{v(k)}$. The order of the VAR process is $p$ and different values of $p$ can be tried or this order can be optimized using a criterion such as the Akaike AIC criterion [25]. The unknown parameters can be estimated using many signal processing methods based on a least squares formulation (i.e. solving the Yule Walker equations). Vector autoregressive moving average (VARMA) processes can also be used as models. Since the models are nonstationary more general vector autoregressive integrated moving average (VARIMA) processes can also be used as models [26].

Standard signal processing is also needed to process data by first segmenting data (restrict to daylight hours) and processing data (lowpass filter and decimation). Then the mean of data at each time can be subtracted along with dividing by deviation of data. Data can then be divided into times when weather is sunny, partly cloudy or cloudy. A detector (detect one of the three states: sunny, partly cloudy, cloudy) can be used to detect transitions to each of the different states. A Markov modulated model can be constructed where the parameters in each state are different and can be estimated using least square methods.

We examined NREL solar data by looking at sensor data taking from Kaleloa, Hawaii [27]. The data consists of 1 second sampled data from 17 sensors. We looked at four sensors that were each several hundred meters from each other and extracted data from December, 2010. The data was first segmented to times between 6:30 AM to 6:30 PM. We then filtered and decimated the signal using a sixty tap rectangular filter and decimated the signal by sampling every fifteen seconds. A plot of the data is shown in Fig. 4.

From Fig. 4 we noted that the four sensor are highly correlated. The correlation between the 15 second samples varies between pairs of samples varies between 0.9345 and 0.9573. The data also shows that most days were sunny or mostly sunny with four cloudy days on Dec. 10, 19, 20, and 27. In Fig. 5 we show three different individual days.

From Fig. 5 we noted that the data is characterized by three regimes: sunny, partly cloudy, and cloudy periods. During sunny and cloudy periods the four sensors are highly correlated and differences between successive samples are relatively small. During partly cloudy periods which is observed during the mid day period of Dec. 1st the fours sensors vary more and differences between successive samples can vary widely.

We then normalized data by looking at each time and subtracting out the 31 day mean at that time for each sensor. We then modeled the data as a VAR(p) process and solved the Yule Walker equations for $p$ ranging from 1 to 100. We plot the root mean squared error for $p$ ranging from 1 to 40 in Fig. 6.

From Fig. 6 we noted that there is only small improvement when $p > 3$ while matrices $A_i$ are all diagonally dominant. This indicates that for prediction the dominant terms are temporal from that given sensor rather than spatial values. As an example if we let $p = 5$ we get that the coefficients rounded to .01 are given by

$$A_1 = \begin{bmatrix} 1.84 & .05 & .02 & .04 \\ .03 & 1.87 & .06 & .03 \\ .01 & -.01 & 1.84 & .07 \\ .04 & -.01 & .06 & 1.85 \end{bmatrix}$$

$$A_2 = \begin{bmatrix} -1.06 & .02 & -.03 & -.02 \\ -.03 & -1.10 & -.08 & -.05 \\ -.02 & .02 & -1.07 & -.10 \\ -.04 & .06 & -.07 & -1.07 \end{bmatrix}$$

$$A_3 = \begin{bmatrix} .21 & -.02 & .01 & -.03 \\ .04 & .17 & .03 & .04 \\ .02 & -.03 & .19 & .05 \\ .04 & -.06 & -.01 & .20 \end{bmatrix}$$

$$A_4 = \begin{bmatrix} -.20 & .02 & .01 & .04 \\ -.03 & .10 & -.01 & -.03 \\ -.01 & .10 & -.13 & .02 \\ 0 & .06 & .06 & -.15 \end{bmatrix}$$

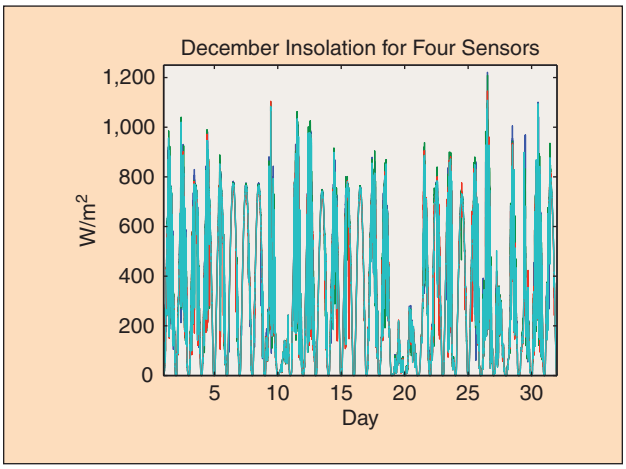


**FIGURE 4** Solar insolation data sampled every 15 seconds.

$$A_5 = \begin{bmatrix} .19 & -.01 & -.01 & -.02 \\ 0 & .13 & .01 & .02 \\ 0 & -.07 & .15 & -.04 \\ -.02 & -.02 & -.03 & .15 \end{bmatrix}.$$

Using the AR(p) model we can then assume that each sensor is conditionally independent of other sensors given temporal data at the $p$ time taps. This makes intuitive sense as during partly cloudy periods the solar insolation can vary widely from sensor to sensor. A more reliable predictor for a particular sensor during partly cloudy periods is based on time lags of that sensor rather than time lags of other sensors.

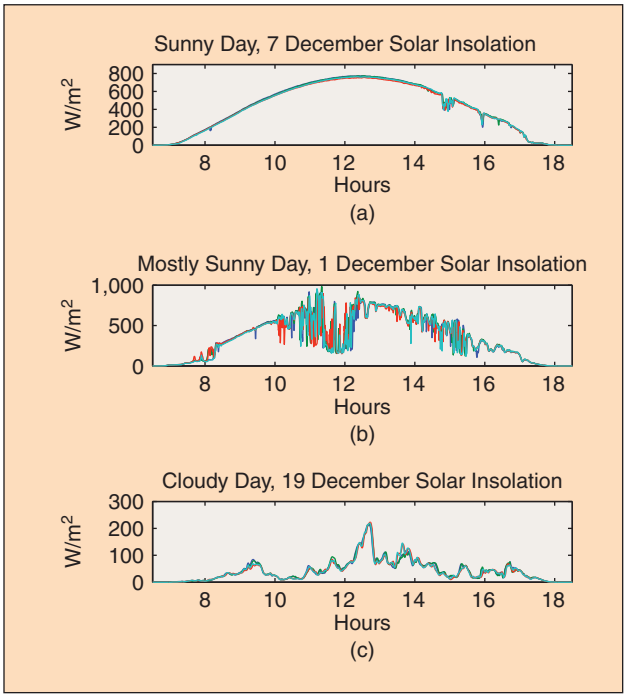


**FIGURE 5** Solar insolation data for four sensors sampled every 15 seconds (sunny day, most sunny day, cloudy day).

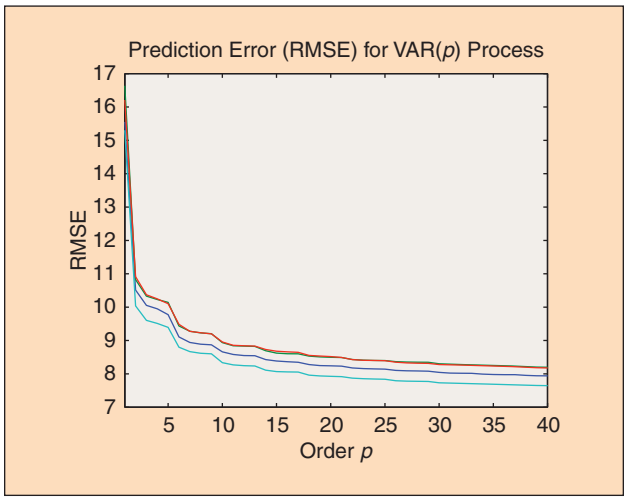


**FIGURE 6** Root mean squared error (RMSE) for VAR($p$) process (This is the one step prediction error.)

Other experiments were conducted by dividing data into slowly varying regimes (sunny and cloudy times) and quickly varying regimes (partly cloudy times). A least squared prediction was done for each of the two regimes and we again observed similar findings that the $A_i$ matrices were again diagonally dominant. We also observed that the overall RMSE was just slightly less than using just one VAR model. We also did $l$ step predictions of the data where $l$ varied from 2 to 10 time steps. The RMSE increased roughly linearly as we increased the prediction time step $l$. Further studies would use online adaptive filters such as the recursive least squares filters to account for the nonstationary data and also using a VARIMA model.

Note that these experiments are preliminary and just describe solar insolation correlations at four different sites over one month. There are seasonal changes and to conduct a comprehensive study data must be observed over a few year period. This must then be correlated to the energy produced by the PV panels. The preliminary study does give some indications of the Markov random field graph that can be constructed showing the nature of temporal and spatial correlations. Other approaches are to use data gathered from sensors such as Locational Monitors (LM1s) to forecast energy produced by the PV panels [28]. The LM1s are reference calibrated small photovoltaic panels that are used by Hawaiian Electric Company and provide more accurate estimates of PV energy than solar irradiance. Another direction is to use standard machine learning approaches such as support vector machines for forecasting [29].

## IV. BP Based State Estimator

### *A. Implementation Algorithm*

The state estimator first works on the network topology through the topology processor. A factor graph model is generated from the bus/branch representation of the grid. Then statistical inference is conducted on the graphical model based on a set of initialization and sparse observations. Fig. 7 compares the difference between the conventional state estimator and the BP based state estimator.

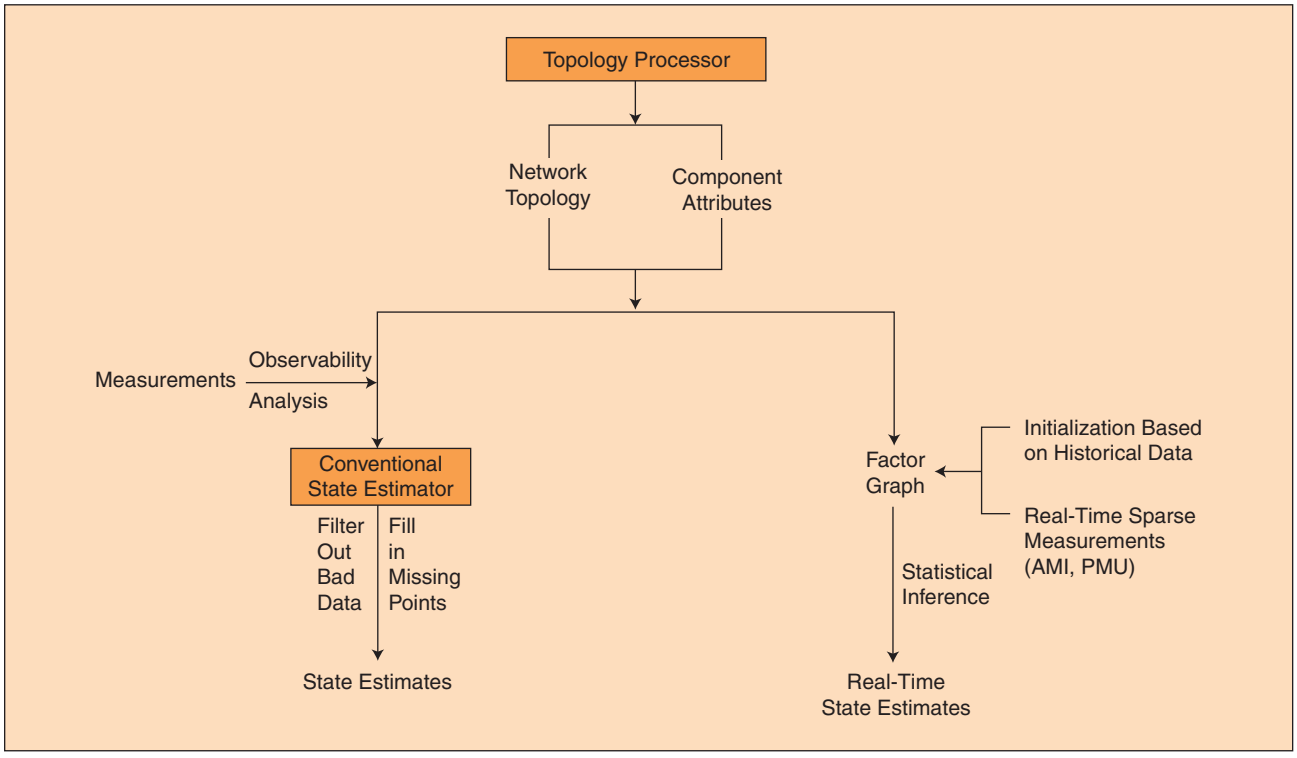


**FIGURE 7** The comparison between conventional state estimator and the BP based state estimator.

For the conventional state estimation, observability analysis should first be conducted to ensure that the measurement equations are solvable. In comparison, there is no need for such analysis in the BP based state estimator. However the prior distribution of all the state variables need to be specified. The accuracy of the state estimates depends both on the initialization accuracy and the amount of observations available. The initialization of the prior distributions also has a great impact on the convergence speed of the algorithm.

**The accuracy of the state estimates depends both on the initialization accuracy and the amount of observations available.**

The prior distribution can be generated from historical readings of the SCADA, AMR or other metering devices. In a distribution network if only kw and kvar readings are available at the injection buses, we can adopt the following two-step approach [4] to derive the initial branch current and bus voltage:

1) Set the voltage values to be 1 p.u. value, then use the injected power reading at every node to calculate the branch current;
2) Use the branch current computed in the previous step and the root bus voltage to calculate all the bus voltages.

The steps of the state estimation algorithm are described in Fig. 8. Section II discussed the measurement update and message passing algorithm in the spirit of the Kalman Filter algorithm.

### *B. Application on Two-Level Distribution Network*

In traditional power system state estimation, all the equipment beyond the substations are modeled as a lump load. Relatively little monitoring and control is available at the feeder circuit level. However, the load variability increases due to the integration of distributed renewable energy generation. The change of the load characteristics can cause serious problems with load modeling and forecasts.

The BP based state estimator can be applied on the power distribution system that starts from the subtransmission system to the consumer's service switches. The distribution system that we are considering includes the subtransmission substation, distribution substation, primary distribution feeders, distribution transformers, secondary circuit including the services to the consumers [30]. This approach supplements the lack of real time system analysis at the feeder circuit level.

We propose a two-level architecture for applying the BP based state estimator in the distribution network topology. Reference [31] presents a two-level infrastructure for utility control and system operation on the distribution grid. As shown in Fig. 9 [31], the first level of monitoring and control can be implemented at the distribution substation. It opens an operational eye on the regional/local behavior at the feeder circuits and enables the correlation analysis between the REG and load characteristics. Then the control center with system operation ability gathers data from the distribution substations through gateway access. At each level, the BP based state estimator can be applied to deliver the system state for further operation and control.

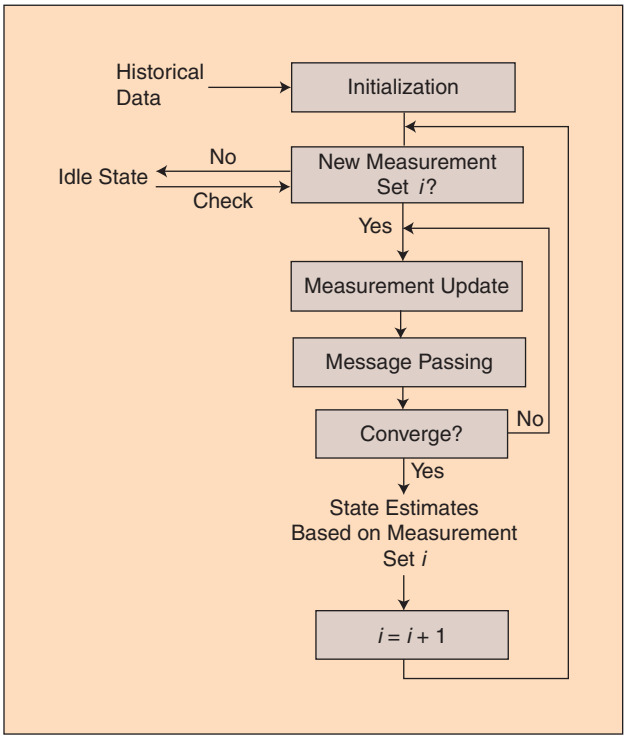


**FIGURE 8** The implementation steps of the BP based state estimation.

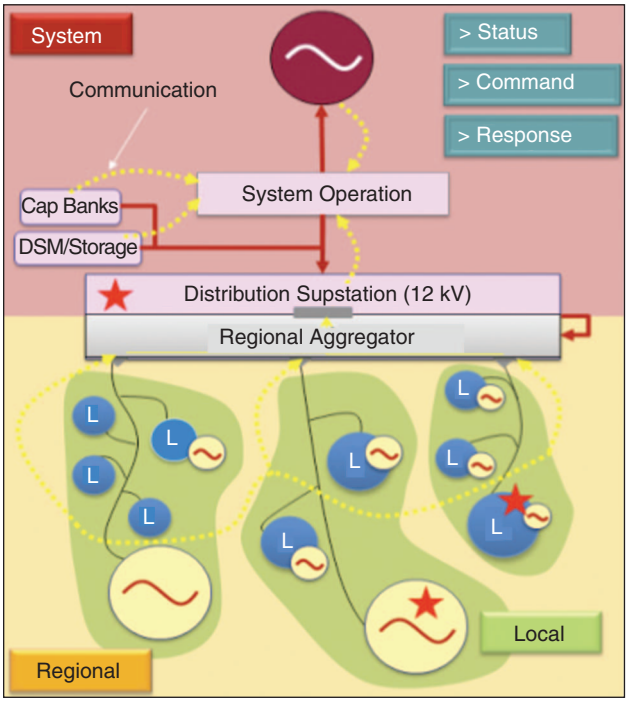


**FIGURE 9** The "smarter" two-level control infrastructure.

**With the two-level architecture the control center only needs to communicate with the substations rather than all the metering devices down to the feeder circuits. The bulk data from meters in the feeder circuits can be stored at the distribution substations. Only the results of the first-level state estimation needs to be transferred to the second-level state estimator.**

The two-way flow of information between the control center and distribution substations has been implemented in some power systems. The traditional state estimation relies on the SCADA system to gather real time measurements from the substations. The communication network that supports SCADA is usually a star connection between the control center and all the substation remote terminal units (RTU). The substation data is gathered by the RTU and polled by the SCADA at every few seconds [32]. If we transfer all the real time measurements in the distribution system via communication network to the control center, the traffic will be a tremendous burden to the control center.

With the two-level architecture the control center only needs to communicate with the substations rather than all the metering devices down to the feeder circuits. The bulk data from meters in the feeder circuits can be stored at the distribution substations. Only the results of the first-level state estimation needs to be transferred to the second-level state estimator [32]–[33]. This approach alleviates the need to transmit the large volume of raw measurements to the control center. System operators at the control center can choose to "zoom in" to look at the detailed feeder behavior beyond the substations.

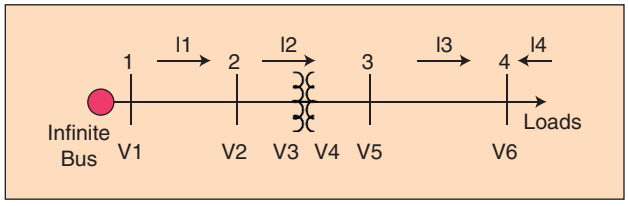


**FIGURE 10** The one-line diagram of distribution feeder circuits.

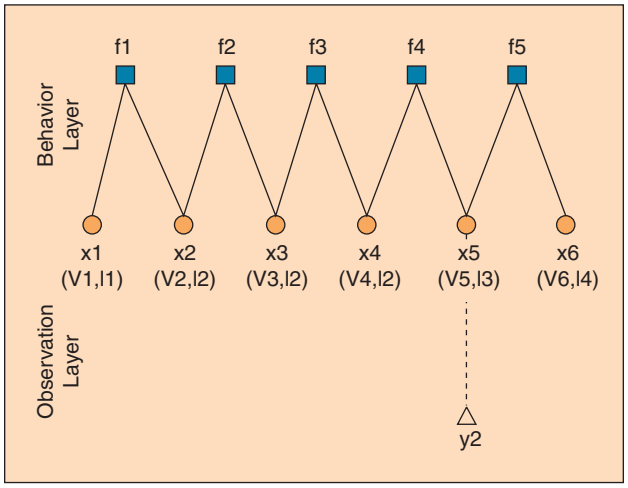


**FIGURE 11** The factor graph model of Fig. 10.

Now we consider the information flow between meters and first-level state estimators, which can include both the meter data and the backward control signals. If the communication network uses a star connection, all the meter data is transmitted directly to the regional state estimator at the distribution substation. If the mesh network is implemented, the meters themselves act as repeaters passing data to nearby meters until it reaches the local computational center [34].

## V. Example

We use the IEEE 4 node test feeder as the test system and its one-line diagram is shown in Fig. 10. Its parameter settings and solutions are listed in [35]. Balanced loading is assumed here so that we can completely decouple the three phases and conduct per phase analysis. The step-down Y-Y transformer brings voltage level from 12.47 KV to 4.16 KV. We conducted per unit analysis with base KVA = 2000K VA for one phase, line-to-ground baseKV = 7.2 kV for high voltage end and line-to-ground baseKV = 2.402 kV for low voltage end.

For comparison we first conducted traditional state estimation using OpenDSS [36]. Load is assumed to have constant active and reactive power. Power flow through the step-down transformer in one phase is at 2000 KVA. During initialization, all the voltages are set to be 1 p.u.

Then the proposed BP state estimator is tested on the same system. Fig. 11 shows the factor graph model of the test feeder.

| **Variable** | V1 | V2 | V3 | V4 | V5 | V6 |
|---|---|---|---|---|---|---|
| **Value** | 1 | 1 – 0.3i | 1 – 0.3i | –0.8 + 0.5i | –0.8 + 0.5i | –0.8 – 0.3i |
| **Variable** | I1 | I2 | I3 | I4 | | |
| **Value** | –1.2 + 0.4i | –1.2 + 0.4i | –1.2 + 0.4i | 1.2 – 0.4i | | |

**FIGURE 12** Initialization of the BP state estimation on IEEE 4 node test feeder.

In the behavior layer, a circle denotes a state vector including two state variables; a square denotes a factor function which may include both $f_E$ and $f_L$. In the observation layer, triangles represent the measurements of the state variables.

On the one-line diagram all the voltages and currents are labeled uniquely as shown in Fig. 10. A topology processor is implemented in the state estimator which converts the system to a factor graph. Essentially the topology processor generates a bipartite graph with all the state variables, factor nodes and a sparse adjacency matrix that defines their connections. Through topology processing, the connection between buses and branches and all the component attributes can be stored in a matrix for each factor function block.

We simulate the BP state estimation algorithm as shown in Section IV.A. As shown in Fig. 3, observations are given with addition of Gaussian noise (zero mean and very small variance). The mean of the state variables are initiated with the p.u. values in Fig. 12. After the first round of convergence, the estimates in every round can be provided as the prior distribution for the next round of state estimation.

**However, BP state estimation utilizes pseudo-measurements as the initialization of prior distributions. With finer initialization, the algorithm can converge to desired estimates even without many real-time measurements.**

Fig. 13 shows the magnitude estimates from both OpenDSS and BP state estimator and can be compared with the benchmark solutions. Fig. 14 is the mean squared error (MSE) of both magnitude and angle estimates from BP state estimation. With OpenDSS we perform the single-snapshot state estimation. The MSE for magnitude estimates is 4.5948e-4 and for angle estimates is 6.5921. In comparison, after one round of BP state estimation, the MSE for magnitude estimates is 4.3545e-4 and for angle estimates is 1.0779e-4.

As shown in the results comparison, BP state estimation performs slightly better with finer initialization on the test feeder. The BP state estimator will show more advantages on distribution network where real-time measurements are very limited. Too many pseudo-measurements may cause the failure of convergence or the convergence on wrong estimates for traditional state estimation algorithm. However, BP state estimation utilizes pseudo-measurements as the initialization of prior distributions. With finer initialization, the algorithm can converge to desired estimates even without many real-time measurements. The REG is not considered on the benchmark system. In our previous work [23] the BP state

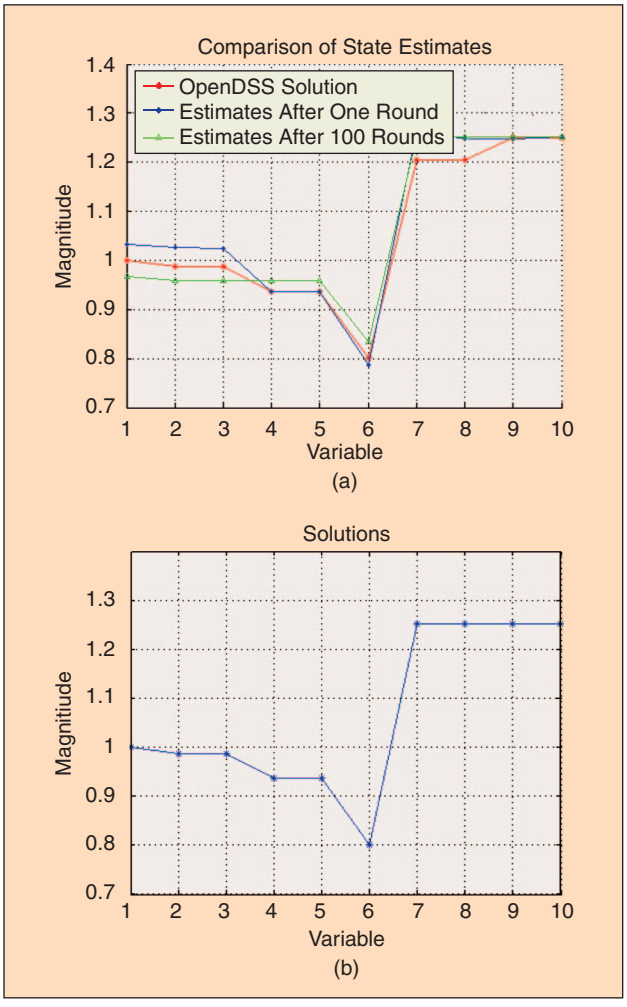


**FIGURE 13** Solutions and state estimates comparison. (a) Results of state estimations and (b) benchmark solutions.

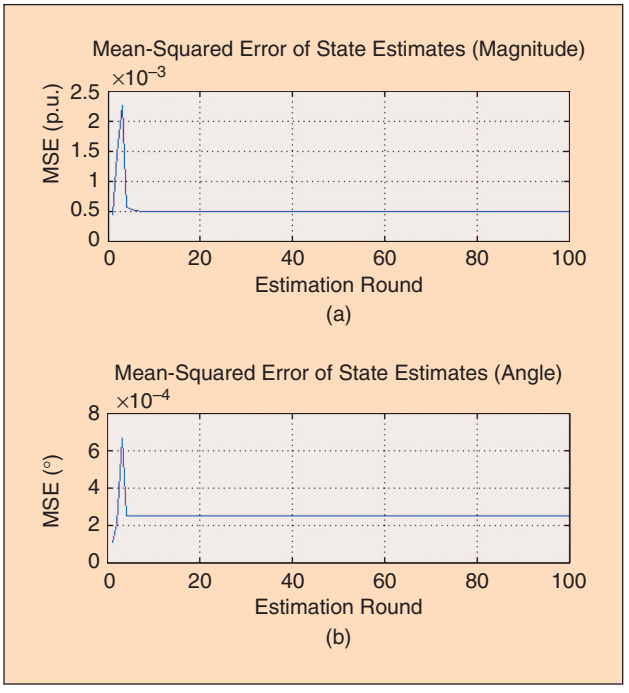


**FIGURE 14** Parts (a) and (b) show the MSE of BP state estimation.

estimation algorithm was tested on two extreme cases of renewable correlation. Further studies need to be conducted to integrate the correlation model discussed in Section III.C.

## VI. Summary and Further Directions

Power system state estimator provides a mathematical model of a power system for advanced control and optimization operations. As the distribution systems have limited amount of measurements, especially at the feeder circuit level, smart grid applications including the distribution automation applications needs this Belief Propagation based state estimator to deal with sparse measurements. The probabilistic inference approach can derive first and second order statistics of the state variables given prior distributions and real-time measurements. This approach also bridges the gap between transmission state estimator and real-time feeder analysis and can be potentially utilized for the implementation of a smart micro-grid.

Preliminary studies have shown some of the correlation and prediction models for temporal and spatial solar insolation data. Further studies are needed on more data to confirm these results and apply this to PV energy generation. With an accurate and timely state estimation result, we could monitor the system performance, determine the optimal meter placement, and diagnose the malfunction of both the monitoring system and the grid. Furthermore, from the models distributed control strategies can be adopted to stabilize the power grid and detect problems occurring on the feeder circuit.

## Acknowledgments

The authors acknowledge the many helpful discussions with Prof. Marija Ilic of Carnegie Mellon University and Dr. Dora Nakafuji of Hawaiian Electric Company Inc. Ying Hu and Anthony Kuh gratefully acknowledge the support from the National Science Foundation under grant NSF-ECCS0938344 and the University of Hawaii Renewable Energy and Island Sustainability (REIS) Program.

## References

[1] A. Abur and A. G. Exposito, *Power System State Estimation: Theory and Implementation*. New York: Marcel Dekker, 2004.

[2] M. E. Baran and A. W. Kelley, "State estimation for real-time monitoring of distribution systems," *IEEE Trans. Power Syst.*, vol. 9, pp. 1601–1609, Aug. 1994.

[3] C. N. Lu, J. H. Teng, and W.-H. E. Liu, "Distribution system state estimation," *IEEE Trans. Power Syst.*, vol. 10, no. 1, pp. 229–240, 1995.

[4] H. Wang and N. N. Schulz, "A revised branch current-based distribution system state estimation algorithm and meter placement impact," *IEEE Trans. Power Syst.*, vol. 19, no. 1, Feb. 2004.

[5] M. E. Baran and A. W. Kelley, "A branch-current-based state estimation method for distribution systems," *IEEE Trans. Power Syst.*, vol. 10, pp. 483–491, Feb. 1995.

[6] F. F. Wu and A. Monticelli, "Network observability: Theory," *IEEE Trans. Power App. Syst.*, vol. 104, no. 5, pp. 1042–1048, May 1985.

[7] A. Monticelli and F. F. Wu, "Network observability: Identification of observable islands and measurement placement," *IEEE Trans. Power App. Syst.*, vol. 104, no. 5, pp. 1035–1041, May 1985.

[8] M. E. Baran and T. E. McDermott, "Distribution system state estimation using AMI data," in *Proc. Power Systems Conf. and Exposition (PSCE'09)*, Seattle, WA, 2009, pp. 1–3.

[9] H. Wang and N. N. Schulz, "A load modeling algorithm for distribution system state estimation," in *Proc. Transmission and Distribution Conf. and Exposition (IEEE/PES)*, 2001, vol. 1, pp. 102–105.

[10] E. Manitsas, R. Singh, B. Pal, and G. Strbac, "Modeling of pseudo-measurements for distribution system state estimation," in *Proc. SmartGrids for Distribution, CIRED Seminar*, June 2008, pp. 1–4.

[11] R. Singh, B. C. Pal, and R. A. Jabr, "Distribution system state estimation through Gaussian mixture model of the load as pseudo-measurement," *IET Gener., Transm. Distrib.*, vol. 4, no. 1, Jan. 2010.

[12] A. P. S. Meliopoulos, G. J. Cokkinides, F. Galvan, and B. Fardanesh, "Distributed state estimator—Advances and Demonstration," in *Proc. 41st Hawaii Int. Conf. Syst. Sci.*, 2008, p. 163.

[13] S. Jakovljevic and M. Kezunovic, "Advanced substation data collecting and processing for state estimation enhancement," in *Proc. IEEE Power Engineering Society Summer Meeting*, July 2002, vol. 1, pp. 201–206.

[14] I. Ben-Gal, "Bayesian networks," in *Encyclopedia of Statistics in Quality and Reliability*. New York: Wiley, 2007.

[15] M. Jordan and T. J. Sejnowski, Eds., "Graphical models: Foundations of neural computation," in *Computational Neuroscience*. Cambridge, MA: MIT Press, 2001.

[16] C. M. Bishop, "Pattern recognition and machine learning," in *Information Science and Statistics*. Berlin: Springer-Verlag, 2006.

[17] F. R. Kschischang, B. J. Frey, and H.-A. Loeliger, "Factor graphs and the sum–product algorithm," *IEEE Trans. Inf. Theor.*, vol. 47, no. 2, Feb. 2001.

[18] G. D. Forney, Jr., "Codes on graphs: Normal realizations," *IEEE Trans. Inform. Theory.*, vol. 47, no. 2, Feb. 2001.

[19] D. Heckerman, "A tutorial on learning with Bayesian networks," *Microsoft Research, Tech. Rep. MSR-TR-95-06*, Mar. 1995.

[20] J. Nunnink and G. Pavlin, "Towards robust state estimation with Bayesian networks: A new perspective on belief propagation," in *Proc. IAS*, 2006, pp. 722–731.

[21] H.-A. Loeliger, J. Dauwels, J. Hu, S. Korl, L. Ping, and F. R. Kschischang, "The factor graph approach to model-based signal processing," *Proc. IEEE*, vol. 95, no. 6, June 2007.

[22] Y. Hu, A. Kuh, A. Kavcic, and D. Nakafuji, "Micro-grid state estimation using belief propagation on factor graphs," in *Proc. APSIPA Annu. Summit and Conf.*, Singapore, Dec. 2010.

[23] Y. Hu, A. Kuh, A. Kavcic, and D. Nakafuji, "Real-time state estimation on micro-grids," in *Proc. IJCNN*, San Jose, CA, July 2011, submitted for publication.

[24] J. Bebic, R. Walling, K. O'Beien, and B. Kroposki, "The Sun also rises," *IEEE Power Energy Mag.*, vol. 7, no. 3, pp. 45–54, May/June 2009.

[25] H. Akaike, "A new look at the statistical model identification," *IEEE Trans. Automat. Contr.*, vol. 19, no. 6, pp. 716–723, 1974.

[26] T. Mills, *Time Series Techniques for Economists*. Cambridge, MA: Cambridge Univ. Press, 1990.

[27] NREL. Solar irradiance website. [Online]. Available: http://www.nrel.gov/midc/

[28] D. Nakafuji, T. Aukai, L. Dangelmaier, C. Reynolds, J. Yoshimura, and Y. Hu, "Back to basics: Operationalizing data mining and visualization techniques for utilities," in *Proc. 2011 IJCNN*, San Jose, CA, July 2011, submitted for publication.

[29] N. Sapankevyeh and R. Sankar, "Time series prediction using support vector machines: A survey," *IEEE Comput. Intell. Mag.*, vol. 4, no. 2, pp. 24–38, 2009.

[30] *McGraw-Hill Encyclopedia of Science and Technology*, 5th ed. New York: McGraw-Hill.

[31] D. Nakafuji, T. Aukai, R. Davis, E. Stewart, J. Keller, and B. Kroposki, "Developing an operational eye for solar," in *Proc. Renewable Energy World Conf.*, Jan. 2011.

[32] T. Yang, H. Sun, and A. Bose, "Transition to a two-level linear state estimator, part I: Architecture," *IEEE Trans. Power Syst.*, vol. 26, no. 1, pp. 46–53, Feb. 2011.

[33] T. Yang, H. Sun, and A. Bose, "Transition to a two-level linear state estimator, part I: Algorithm," *IEEE Trans. Power Syst.*, vol. 26, no. 1, pp. 54–62, Feb. 2011.

[34] V. C. Gungor and F. C. Lambert, "A survey on communication networks for electric system automation," *Comput. Netw.*, vol. 50, no. 7, pp. 877–897, May 2006.

[35] IEEE Distribution Planning Working Group Report, "Radial distribution test feeder," *IEEE Trans. Power Syst.*, vol. 6, no. 3, pp. 975–985, Aug. 1991.

[36] Wiki Documentation [Online]. Available: electricdss.wiki.sourceforge.net